Journal of Infrastructure Intelligence and Resilience 3 (2024) 100107

Contents lists available at ScienceDirect

Journal of Infrastructure Intelligence and Resilience

journal homepage: www.journals.elsevier.com/journal-of-infrastructure-intelligence-and-resilience

Advancement of data-driven SHM: A research paradigm on AE-based switch rail condition monitoring

Lu Zhou [a], Si-Xin Chen [b,*], Yi-Qing Ni [c,d], Xiao-Zhou Liu [e]

[a] School of Civil Engineering, Sun Yat-Sen University, Zhuhai, Guangdong, China
[b] Department of Civil Engineering and Smart Cities, Shantou University, Shantou, Guangdong, China
[c] Department of Civil and Environmental Engineering, The Hong Kong Polytechnic University, Hung Hom, Kowloon, Hong Kong S.A.R, China
[d] Hong Kong Branch of National Transit Electrification and Automation Engineering Technology Research Center, Hung Hom, Kowloon, Hong Kong S.A.R, China
[e] College of Urban Transportation and Logistics, Shenzhen Technology University, Shenzhen, Guangdong, China

ARTICLE INFO

Handling editor: Ms. Yanwei Li

Keywords:
Structural health monitoring
Railway engineering
Infrastructure intelligence
Acoustic emission
Data analytics
Transfer learning

ABSTRACT

The past ten years have witnessed the tremendous progress of structural health monitoring applications in civil infrastructures. This is particularly embodied in railway engineering. The increasing train speed brings greater challenges to safety and ride comfort, and the primary theme of maintenance has been gradually altered from offline inspection to online monitoring. Rail operators must get an in-time warning of potential structural defects before critical failure takes place. It is more favourable that the rail operators can take hold of the real-time status of the key components and infrastructures in railway systems. This paper summarizes a long-term research series by the authors' research team on online monitoring of rail tracks at turnout areas utilizing acoustic emission-based sensing technique, and more importantly, successively advancing signal processing methods and data-driven analysing frameworks, covering Bayesian inference, convolutional neural networks, transfer learning and task similarity analysis. The proposed algorithms tackle noise interference brought by wheel-rail impacts, great uncertainties in an open environment, and insufficiency of monitoring data, and realize comprehensive monitoring of rail tracks in turnout areas from basic crack detection to regressive condition assessment step-by-step.

1. Introduction

The rail track is the key component in railway systems, any small crack or flaw in the rail may bear great risk to safety operation, disrupting train services (The Associated Press, 2021) and yielding potential catastrophic consequences (derailment) (Dimsumdaily Hong Kong, 2019), threatening life and economy. In-time and regular inspection of rail is therefore essential to check the structural integrity of rail structure. Ultrasonic testing, as a superior non-destructive evaluation (NDE) method, has been extensively adopted in rail inspection. By emitting and receiving ultrasonic signals of either transmission, reflection, refraction, scattering, etc., structural discontinuities (hollows, cracks, delamination and so on) can be referred to through analysis in time and frequency domains. The most common ultrasonic testing technique used for rail inspection is the ultrasonic phased array, which contains an array of ultrasonic sensing elements to emit ultrasonic waves with pre-controlled phase shift, forming wavefronts in various angles, and enabling imaging of a plane. The ultrasonic phased array normally appears as a hand-held device and is primarily used for diagnosing flaws in rail sections, including near-surface cracks (Anandika et al., 2020), transverse flaws (Benzeroual et al., 2021), and rail welds (Xu et al., 2021a,b). Different approaches have also been proposed to enhance the imaging quality from phased arrays (Kim et al., 2020; Utrata, 2002). With the rapid development of high-speed rail (HSR), offline manual inspection through ultrasonic phased arrays cannot fully guarantee operating safety and it is online structural health monitoring (SHM) with in-time alerts of early structural defects that is most needed. Concerning the rail structure is naturally a good waveguide, ultrasonic guided waves-(UGWs-) based technique, under this background, have been profoundly studied in terms of the UGWs propagation mechanism as well as their interaction behaviours with cracks or hollows in rail. Compared to ultrasonic phased array testing, UGWs have a considerably larger sensing range and enable online monitoring of rail tracks by attaching semi-permanent sensing wafers or transducers onto the structure.

* Corresponding author.
E-mail address: chensixin@stu.edu.cn (S.-X. Chen).

https://doi.org/10.1016/j.iintel.2024.100107
Received 8 April 2024; Received in revised form 6 June 2024; Accepted 28 June 2024
Available online 7 July 2024

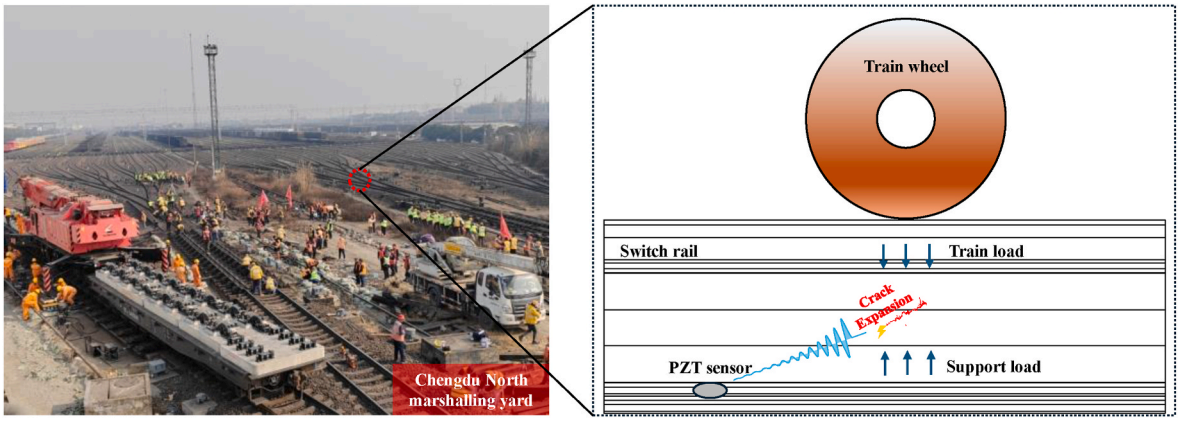

Fig. 1. Rail turnout in Chengdu North marshalling yard.

Among these studies, PW loveday contributed a series of pioneering and valuable work from theoretical research to finite element simulation using semi-analytical methods, and to field tests (Loveday, 2009, 2012; Loveday et al., 2018, 2020; Ramatlo et al., 2018). Francesco Lanza di Scalea also conducted comprehensive research on SHM of rail structures using ultrasounds including propagation modelling of UGWs in arbitrary cross-section (Bartoli et al., 2005, 2006), experimental study of guided waves with various signal processing methods and in-situ measurements (Coccia et al., 2011; di Scalea and McNamara, 2004), and noncontact air-coupled UGWs inspection of rails (di Scalea and McNamara, 2003; Mariani et al., 2013; Mariani and di Scalea, 2018). The UGWs in rail are commonly excited and captured using piezoelectric lead titanate zirconate (PZT) sensors (Ge et al., 2022), while lasers (Ng et al., 2022; Wang et al., 2023a,b) and electromagnetic acoustic transducers (EMATs) (Fan et al., 2007; Hu et al., 2021) are also adopted in some situations to generate guided waves. Regarding the switch rail to be mainly discussed in this paper, recently there have been some pilot studies on the detection of rail defects with ultrasonic shear horizontal (SH) waves and lamb waves (Chen et al., 2021a,b; Li et al., 2023; Wu et al., 2018).

While UGWs-based techniques have been extensively investigated in rail monitoring, the complex dispersion mechanism of guided waves in rail hinders its practical applications. The massive dispersed modes tend to overlap with each other in the time domain, making it tricky to extract a specific mode of interest for further damage-sensitive analysis. For switch rails with more irregular cross-sectional profiles, the dispersion curve can be more sophisticated, which is why the research by (Chen et al., 2021a,b; Li et al., 2023; Wu et al., 2018) is still at the lab experiment and simulation stage. Moreover, UGWs propagate diffusely along the rail elongational direction, and conventional sensing path analysis cannot be directly applied (Wang et al., 2020a,b). In contrast to the active sensing philosophy of UGWs, acoustic emission (AE) as a passive ultrasonic sensing technique, has experienced growing applications in rail defect detection (Bruzelius and Mba, 2004; Hao et al., 2021; Zhang et al., 2014, 2015; 2021). AE refers to the sound burst event generated when structures suffer from irreversible structural change such as crack expansion, the generated AE burst would propagate in the structure. By passively capturing the AE signal, the crack and be detected correspondingly. The biggest merit of AE-based monitoring over UGWs is that it does not require analysis of the dispersion mechanism of ultrasounds and can be easily applied for crack detection only through data processing on the collected acoustic measurements. This makes AE monitoring particularly suitable for switch rails, on which our sensing solution to be reviewed in this paper was established, and in recent years there have been also multiple research articles on this topic (Kongpuang et al., 2022; Rubio-González et al., 2023; Xu et al., 2017; Zhang et al., 2016a,b).

Although crack-induced AE bursts can be easily captured and viewed in the time domain under a lab environment, in real operating rail lines however, the AE bursts are often obscured by the intense vibrations caused by wheel-rail interactions. It is also the wheel-rail impacts that can impel the crack expansion process, which means in most cases the AE bursts must be collected at the very time when a train passes by. These wheel-rail interactions are usually manifested as broadband vibrations, especially in rail turnout areas involving train braking and accelerating, the frequency spectrum can extend to ultrasonic range, hence conventional filtering may be inadequate to identify the signal of interest. This issue also occurs in other AE-based monitoring scenarios, and therefore advanced signal processing approaches or data-driven frameworks, e.g., support vector machine (SVM) (Elforjani & Shanbr, 2017; Wu and Li, 2022), mode decomposition (Li & Xu, 2022; Xu et al., 2020), particle swarm optimization (Li et al., 2017; Xu et al., 2021a,b), deep learning (Barile et al., 2022; Han et al., 2021) and many more have been incorporated to aid fault diagnosis.

This paper summarizes a consecutive long-term research series conducted by the authors and corresponding research team, aiming at online monitoring of rail structural conditions based on AE sensing techniques. The summary of existing works naturally leads to a novel transfer learning (TL) method guided by task similarity (TS), which can not only evaluate the crack stages in a progressive manner but also provide a solid criterion for selecting a proper source model for TL. This is one of the novelties of this study. The research project is presented chronologically from solution proposal and pilot lab test verification to time-frequency analysis for basic and preliminary detection of damage, followed by the development of novel algorithms under state-of-the-art data-driven frameworks including Bayesian inference, neural networks and TL. Through the research series, we progressively reach a more robust, reliable, and generalizable switch rail monitoring solution which has been put into service on multiple operating rail turnout zones, realizing real-time condition assessment of rail tracks in turnout areas. The present study to a certain extent serves as a representative case reflecting the advancement of computer-aided SHM in recent years.

2. AE-based monitoring system and deterministic crack detection with time-frequency analysis

The study was initiated upon a request proposed by China Swjtu Railway Development (CSRD) Co., Ltd. in Chengdu, Sichuan Province, China, concerning a freight line in the Chengdu North marshalling yard (Fig. 1), where the point rails in the turnout area were frequently damaged subject to continuous loading and impacts of passing freight trains, causing fractures and failures. The rail turnout was regularly examined through manual inspection which is time-consuming and cannot provide structural condition information during operating hours, and an online monitoring platform is highly desired to enable in-time alert of early cracks before they develop into critical failures. This puts forward the proposal for our AE-based monitoring system.

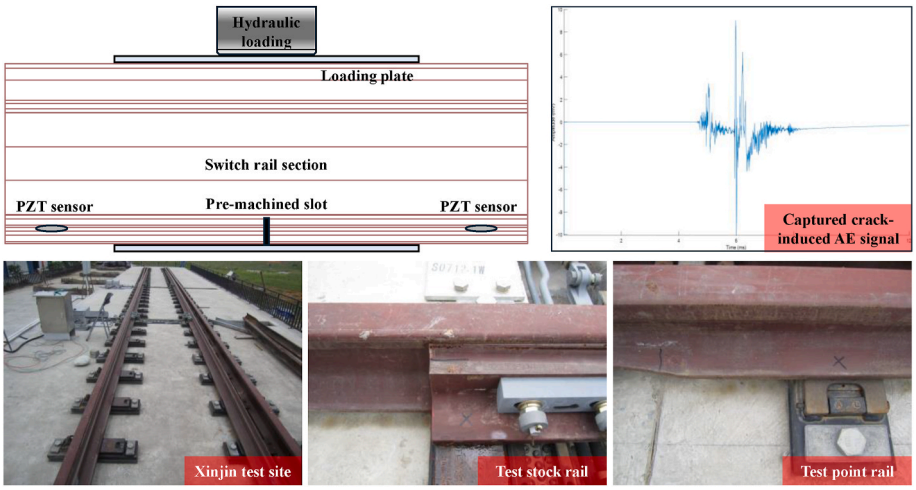

Fig. 2. Feasibility experiment at Xinjin test site.

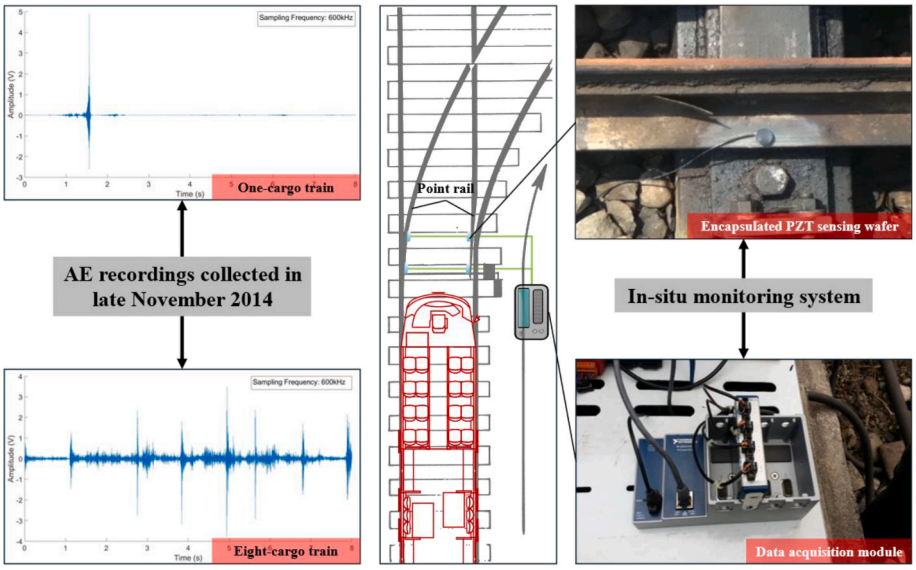

Fig. 3. In-situ monitoring system and AE data examples.

Prior to in-situ monitoring, a series of feasibility experiments were conducted at the Xinjin test site. A stock rail section and a point rail section (1600 mm long) were tested respectively, as illustrated in Fig. 2. An 80 mm deep slot was pre-machined at the rail foot in the middle of the rail section to accelerate the process of fatigue crack initiation and expansion. The rail section was clamped on the test rig with two loading plates placed on top and bottom. Two PZT sensors were implemented at the rail foot equal-distantly 600 mm away from the slot. A hydraulic loading machine was used to apply normal load onto the test rail from 30 kN to 500 kN at a 5 kN loading step and repeat the loading cycle until the rail crack sound was heard. Acoustic measurements were collected during the entire process. As shown in the top left of Fig. 2, the crack-induced AE signal was successfully captured by the PZT sensor and manifested as a solitary peak in the time domain.

The in-situ AE-based monitoring system was implemented at the trackside of a rail turnout of the freight line close to the station, with two PZT sensing wafers mounted on each of the two-point rails which were most vulnerable to external impacts, 3 m and 4 m from the rail tip, as shown in Fig. 3. Since operating rail lines are in an open environment, the PZT sensors were encapsulated to be immune to rainy or snowy weather which may cause malfunctioning. The data acquisition part consists of a four-channel National Instrument 9223 Pickering card and a laptop computer. During the pilot test, the crack-induced AE bursts were found to be mainly located within the 20 kHz–300kHz range, and the sampling rate of the monitoring system was set to 600 kHz. Upon each passing freight train, the monitoring system took 8-s-long recordings from the PZT sensors. The monitoring started at the beginning of September 2014 and lasted three months. The two-point rails had been confirmed intact through manual routine inspection in early October, and a severe fracture with an obvious crack opening was found on one point rail in late November. Examples of AE recordings in late November can also be viewed on the left side of Fig. 3. Because the rail turnout lies in the marshalling yard, either a one-cargo train or an eight-cargo train would pass over the area. The peaks shown in the A-scans do not reflect crack-induced AE bursts, but the impacts by passing wheel-sets since PZT sensors also capture vibrations below 20 kHz. These broadband wheel-rail interactions have much higher vibration amplitudes last much longer time than crack expansions, and completely cover any crack-induced AE bursts in both time and frequency domains even for severe damage. Therefore, filtering is necessary but cannot solely extract the signal of interest and further data processing is essential to deliver a damage-sensitive index for crack detection.

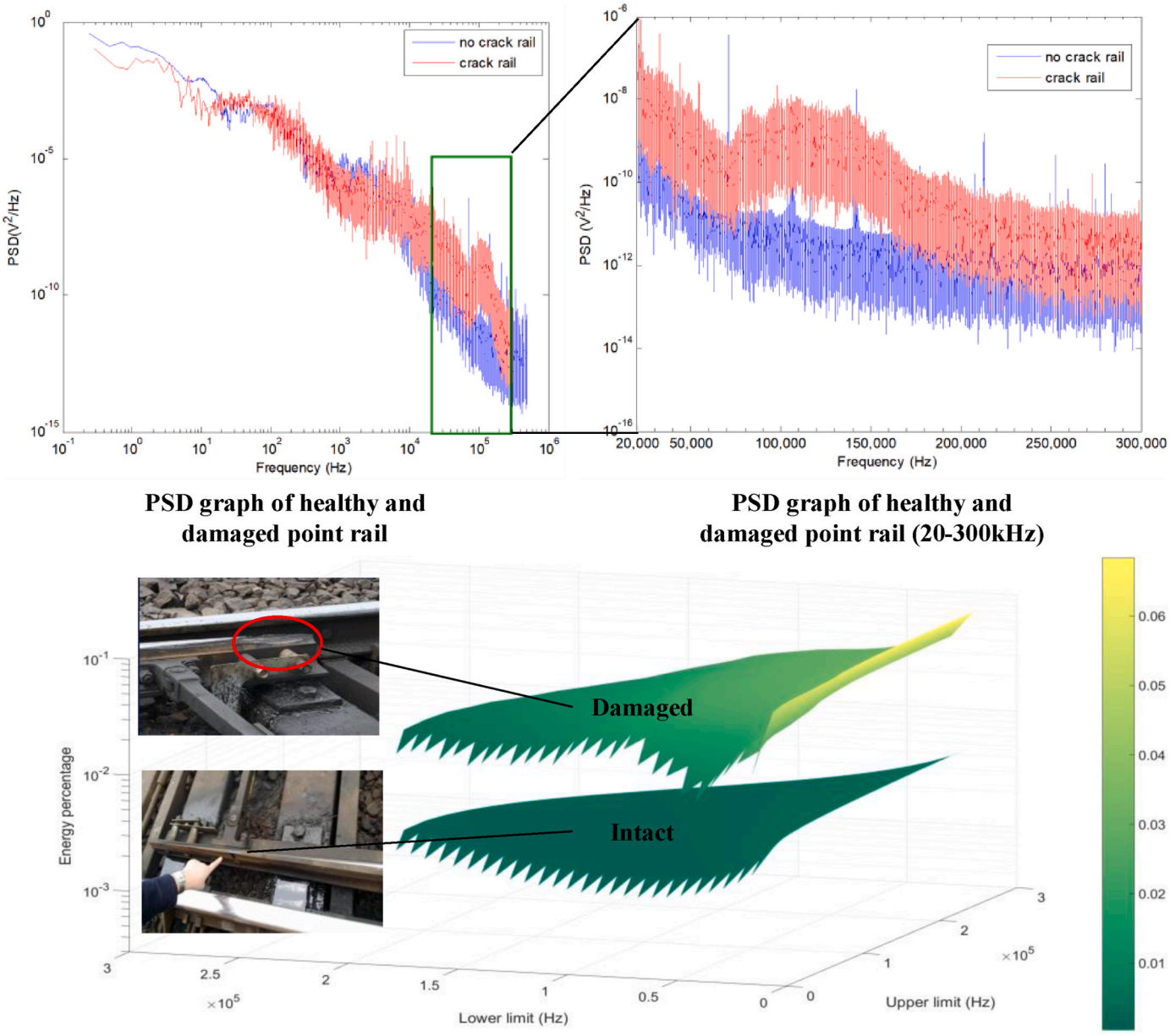

Fig. 4. PSD and patterns of AE measurements from point rail at healthy and damaged states.

Therefore, the authors' research team proposed a damage-sensitive pattern based on the power spectrum density (PSD) (Liu et al., 2015).

The collected signals were firstly processed through a discrete Fourier transform (DFT), band-pass filtering (BPF) and inverse fast Fourier transform (IFFT) process, as listed in Eq. (1), obtaining a filtered signal within the frequency band (f_l, f_u).

$$\begin{cases} X_k = \sum_{s=0}^{n-1} x_s W^{sk}, (DFT) \\ Y(k, f_l, f_u) = H_k X_k, (BPF) \\ y(s, f_l, f_u) = \sum_{k=0}^{n-1} Y(k, f_l, f_u) e^{j2\pi ks/N}, (iFFT) \end{cases} \quad (1)$$

Root mean square (RMS) values were calculated based on the filtered signal as:

$$R(f_l, f_u) = \sqrt{\frac{1}{n-1}\sum_{s=0}^{n-1}\left[y(s, f_l, f_u) - \frac{1}{n}\sum_{s=0}^{n-1} y(s, f_l, f_u)\right]^2} \quad (2)$$

The damage-sensitive feature of each given frequency band (f_l, f_u) is defined as the ratio between the RMS of selected band and the original signal, representing the energy percentage.

$$P(f_l, f_u) = \frac{R(f_l, f_u)}{R_x} \quad (3)$$

An upper triangular pattern matrix is formulated to reduce the computational cost by permutating all the frequency ranges with a minimum interval Δf:

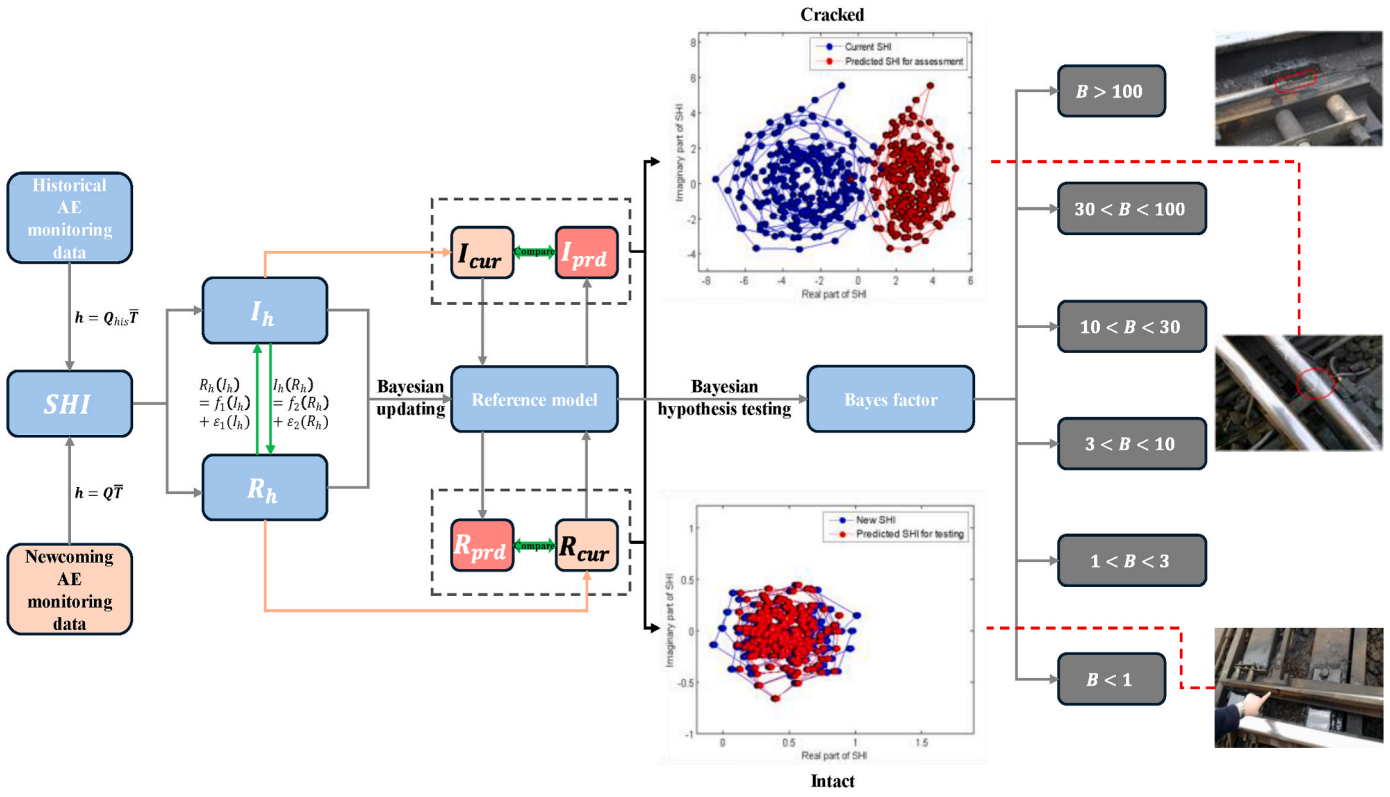

Fig. 5. Flowchart of AE-based probabilistic rail turnout crack diagnosis under Bayesian framework.

$$\boldsymbol{P} = \begin{pmatrix} 0 & P(f_1,f_2) & P(f_1,f_3) & \cdots & P(f_1,f_m) \\ 0 & 0 & P(f_2,f_3) & \cdots & P(f_2,f_m) \\ 0 & 0 & 0 & \cdots & P(f_3,f_m) \\ \vdots & 0 & 0 & \ddots & \vdots \\ 0 & 0 & 0 & \cdots & 0 \end{pmatrix} \tag{4}$$

where $f_1 = 20kHz, f_m = f_s/2$, and $m = \frac{f_2 - f_1}{\Delta f} + 1$, and finally the patterns under healthy and damaged states in a statistical manner can be obtained by taking averages of all patterns under the corresponding state:

$$P_{avg} = \frac{1}{N_{I/D}} \sum_{i=1}^{N_{I/D}} P_i \tag{5}$$

AE measurements collected in early September representing a healthy state and those in late November representing a damaged state were used for PSD and damage-sensitive pattern calculation, plotted in Fig. 4.

As can be seen from Fig. 4 the PSD graph reflects a noticeable but tiny difference between healthy and damaged states specifically within the ultrasonic range, and more obvious distinguishment can be observed in the damage-sensitive patterns. The conventional data processing method enabled a basic binary classification detecting the existence of damage, but it is significant only when the damage is severe and the uncertainties under the open environment are not considered. For more complicated situations and more subtle cracks, further data-driven analysis is needed.

3. Probabilistic crack diagnosis under Bayesian inference

While conventional time-frequency analysis can diagnose the existence of severe damage, the in-situ SHM data, however, is always accompanied by great uncertainties (temperature, weather, noise, etc.), and AE measurements are no exception. AE bursts induced by early small cracks can be more easily influenced by these uncertainties and are likely to either miss the damage or cause false alarms. Bayesian framework has been proven to be an excellent tool for quantifying uncertainties and has met growing applications in SHM for civil infrastructures including bridges (Ni et al., 2020; Ni and Chen, 2021; Sousa et al., 2020), high-rise buildings (Wang et al., 2022; Zeng et al., 2023; Zhang et al., 2016a,b), wind turbines (Jaramillo et al., 2022; Mao and Todd, 2016; Nielsen et al., 2021), and railway systems (Ni and Zhang, 2020; Wang et al., 2023a,b; Wang et al., 2020a,b). The primary merit of Bayesian inference is that it enables the construction of a data-driven model which can be updated continuously with incoming SHM data, and so is the related uncertainty, giving a probabilistic posterior estimation of data distribution and damage diagnosis. A nonparametric approach combining Bayesian regression and Bayes factor was developed by the authors' research team (Wang et al., 2018). A structural health index (SHI) is proposed based on the philosophy that any structural change with be reflected by the dynamic response in the frequency domain, which in this context refers to the frequency spectrum of the AE monitoring data, or more specifically, the relationship between the real part and the imaginary part of the frequency spectrum. The SHI $\boldsymbol{h}$ is constructed through the following equation series:

$$\begin{cases} \boldsymbol{Q}_{his}\boldsymbol{T} = \boldsymbol{S} \\ \overline{\boldsymbol{T}} = \left(\boldsymbol{Q}_{his}^{*}\boldsymbol{Q}_{his}\right)^{-1}\boldsymbol{Q}_{his}^{*}\boldsymbol{S} \\ \boldsymbol{h} = \boldsymbol{Q}\overline{\boldsymbol{T}} \end{cases} \tag{6}$$

where $\overline{\boldsymbol{T}}$ is a numerically computed transformation matrix that can project any historical data $\boldsymbol{Q}_{his}$ or new data $\boldsymbol{Q}$ into the complex-value $\boldsymbol{h}$ with real part R_h and imaginary part I_h, with proposed mutual relationships expressed as:

$$\begin{cases} R_h(I_h) = f_1(I_h) + \varepsilon_1(I_h) \\ I_h(R_h) = f_2(R_h) + \varepsilon_2(R_h) \end{cases} \tag{7}$$

where $f(x) = \sum_{k=1}^{L} \omega_k \varnothing(x_h, x_{h\_k}) = \boldsymbol{\Phi}^T\boldsymbol{\omega}$ is a linear combination of Gaussian distribution functions with $\boldsymbol{\omega}$ being the model parameters to be

updated through Bayesian inference. $\varepsilon(x)$ is random noise, following Gaussian distribution and serving as residuals to be updated. The target $R_h(I_h)$ or $I_h(R_h)$ obey a normal distribution as $N(\mathbf{\Phi}^T\boldsymbol{\omega},\sigma^2)$, and the prior distribution of, the weight factor is also assumed to be Gaussian as $N(\mathbf{0}, \tau^2\mathbf{I})$. Concerning the conjugate prior distribution under the Bayesian inference framework, the prior of the variance τ^2 with zero-mean is an inversion Gamma distribution. By updating with monitoring data through Bayes' theorem, the posterior distribution $N\left(\mathbf{v}_p, \boldsymbol{\tau}_p^2\right)$ of $\boldsymbol{\omega}$ can be obtained, and the corresponding $f_1(I_h)$ and $f_2(R_h)$ can be expressed as:

$$f_{prd}(I_h / R_h) = \mathbf{\Phi}^T\mathbf{v}_p \tag{8}$$

When the imaginary part and real part of a SHI (I_{cur} and R_{cur}) from new coming data are fed to the reference model based on the prediction function f in Eq. (7), predictions of the associated real part and imaginary part (I_{prd} and R_{prd}) can obtained through Eq. (8), and the residuals between predictions and in-situ AE data will be evaluated through a Bayesian hypothesis testing process, yielding a Bayesian factor as:

$$B = exp\left[-\frac{1}{2}ln(n+1)+\frac{n^2\mu_{av}^2}{2(n+1)\lambda^2}\right] \tag{9}$$

A Bayesian factor larger than 1 will be treated as a damaged state and further classified based on the value, otherwise it is inferred to be healthy. Applying the proposed Bayesian approach to the AE monitoring data, the damages can be diagnosed and even quantified through the $I_h - R_h$ relationship model trained from historical monitoring data, as shown in Fig. 5. When the rail is intact, the predicted SHI and current SHI do not have remarkable differences in terms of $I_h - R_h$ relationship. When the rail is cracked, the predicted SHI and current SHI exhibit distinct separation from each other. By leveraging Bayesian inference, a well-trained model can diagnose damage quantitatively in a probabilistic manner based on the derived Bayes factor, while not necessarily requiring any analysis of physical mechanism in advance. Furthermore, the model can be progressively updated upon continuously incoming new data. It should be noted that such a data-driven model relies heavily on adequate data amount, and a limited amount of monitoring data collected under a damaged state would significantly lower the confidence of diagnosis. However, in practical situations, SHM data, especially well-labelled data samples are not always sufficient for model training and testing. This issue directly puts forward to the further advancement of our research, which will be elaborated in the next section.

To further quantify the uncertainties, posterior probabilities $P(H_1|\mathbf{D})$ and $P(H_0|\mathbf{D})$, which represents with and without damage respectively, are calculated through prior knowledge of $P(H_1)$ and $P(H_0)$ based on new monitoring data $\mathbf{D}$ through the following equations:

$$\begin{cases} P(H_1|\mathbf{D}) = \dfrac{B'B}{1+B'B} \\ P(H_0|\mathbf{D}) = 1 - P(H_1|\mathbf{D}) = \dfrac{1}{1+B'B} \end{cases} \tag{10}$$

where B' is the new Bayes factor calculated from Eq. (9) upon new coming data. The metric provides a straightforward way to calculate uncertainties, which helps to optimize the structural maintenance strategy.

Since two Bayes factors can be obtained from Eq. (7), i.e., B_R for $R_h(I_h)$ and B_I for $I_h(R_h)$, the selection criteria can be set as either choosing the maximum value between the two or leveraging the weighted value as:

$$\begin{cases} B_f = \max(B_R, B_I) \\ B_f = (w_R B_R + w_I B_I)/w \end{cases} \tag{11}$$

where $w = w_R + w_I$, $w_R = \left\|\mathbf{R}_{his} - \mathbf{f}_{his}\right\|^{-1}$, and $w_I = \left\|\mathbf{I}_{his} - \mathbf{f}_{his}\right\|^{-1}$. Here $\left\|\mathbf{R}_{his} - \mathbf{f}_{his}\right\|$ and $\left\|\mathbf{I}_{his} - \mathbf{f}_{his}\right\|$ are the Euclidean norm of modelling errors resulting from the training process.

4. Regressive crack evaluation with acoustic TL

As stated in the previous section, when making use of "Big Data" in SHM scenarios, the collected data, especially labelled data is not always "Big" enough to produce a well-trained model. Regarding the AE monitoring case in our project, the monitoring period at Chengdu North marshalling yard lasted three months, with an average of 20 freight trains passing by every day. The data size of each 8-s AE recording at a 600 kHz sampling rate is 36 Mb (4.8 million samples). Eventually, all four PZT sensors collected around 270 Gb for the entire three months, which is far less than the amount in conventional big data analysis disciplines, such as social networks or traffic flow prediction, let alone the AE data collected under damaged states. Apart from Bayesian

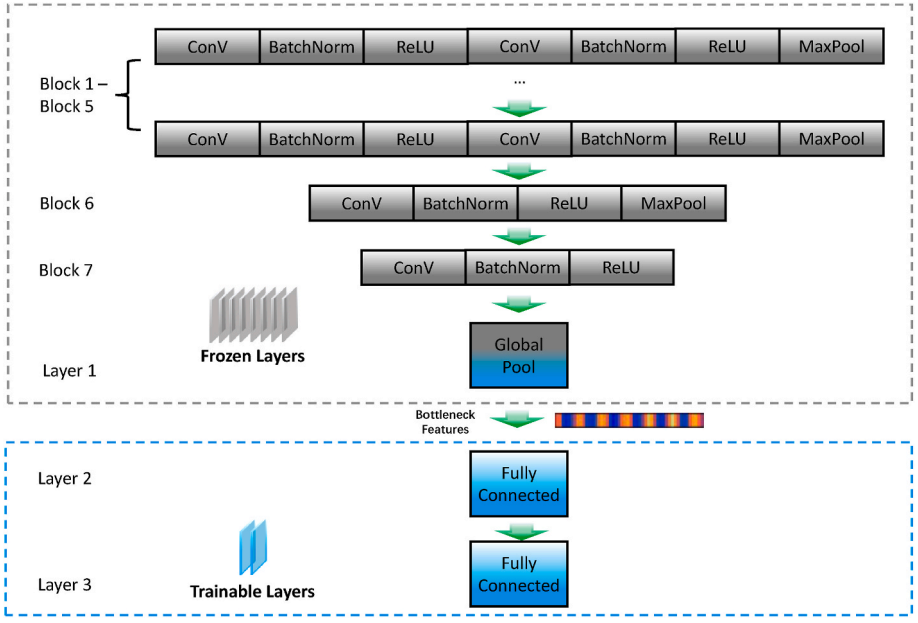

Fig. 6. Architecture of model for crack assessment.

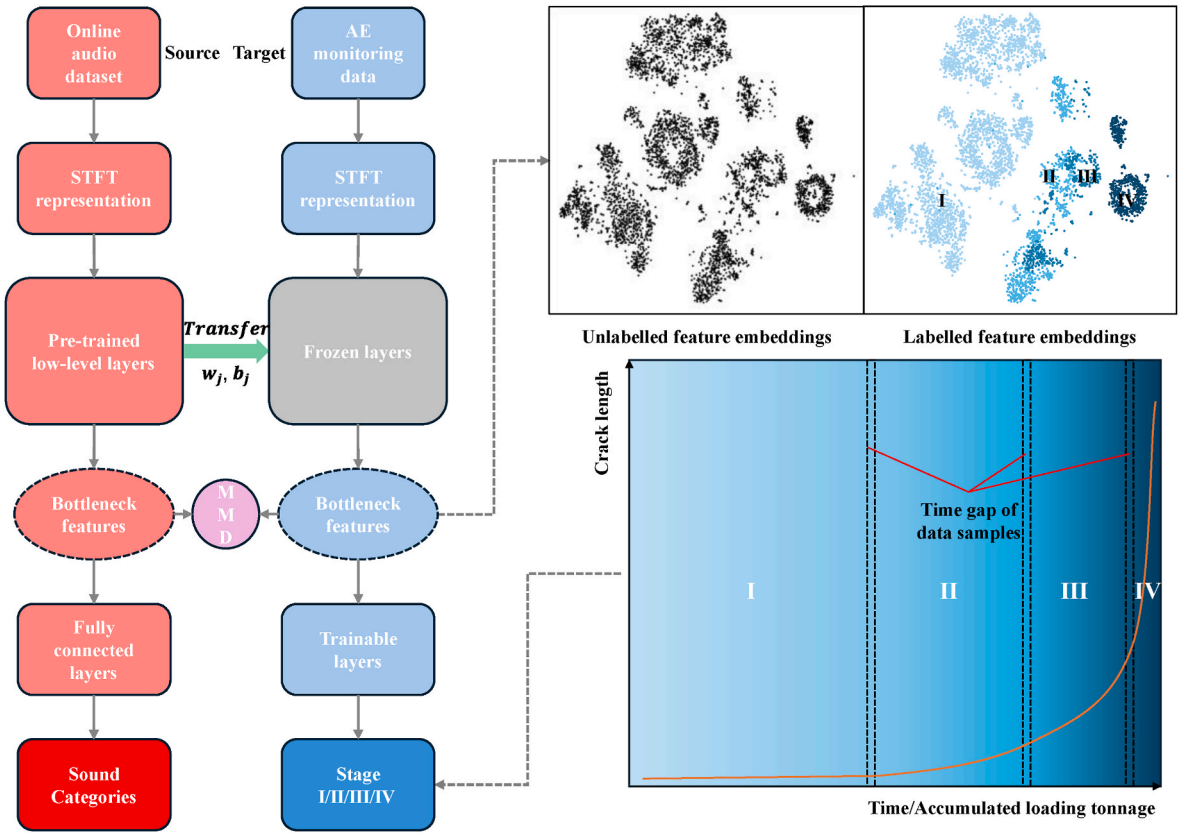

Fig. 7. Flowchart of TL for AE-based rail condition assessment and visualized features of $M_{A\text{-}AE}$.

inference, deep learning models, especially convolutional neural networks (CNNs) are commonly applied for structural damage detection (Ahmadzadeh et al., 2024; Khodabandehlou et al., 2019; Li et al., 2022; Seventekidis et al., 2020; Sony et al., 2021; Zhang et al., 2022). The inadequacy of data amount would lead to the overfitting issue, which is particularly frequent in computer-aided SHM for civil infrastructures including railway systems under open operating environments. In recent years, TL has experienced astonishing outbursts in SHM (Figueiredo et al., 2023; Pan et al., 2023; Rai and Mitra, 2022; Sawant et al., 2023; Ye et al., 2022, 2024). Although still based on the CNN, TL enables knowledge transfer from pre-trained models to the model corresponding to new SHM data, so that data insufficiency can be compensated, and overfitting issues avoided. The pre-trained model can be trained on open-access datasets, finite element simulations or historical data collected under different circumstances. By adopting TL, the damage diagnosis and health assessment can be significantly improved.

In the face of the limited AE monitoring data in this study, we proposed a TL approach to increase the rail condition assessment accuracy (Chen et al., 2021a,b) by leveraging pre-trained models from the AudioSet (Gemmeke et al., 2017), which contains around 2.1 million 10-s audio recordings for 527 sound events, each of which at least contains 59 samples.

In TL, especially inductive TL, it is required that the source task is similar to the target task (Pan and Yang, 2010; Wang et al., 2019) and the lack of similarity between source task and target task may deteriorate the model performance, which is known as "negative transfer". Therefore, before TL, the source task should be carefully analyzed to ensure that it is close to the target task. It can be realized that the task of AE-based crack monitoring is, in essence, to identify the AE of interest out of the complex acoustic scenes, which is similar to the task of detecting the sound event of interest out of the noisy background (other sound events). This preliminary analysis ensures positive knowledge transfer in the first case. In comparison, the task of image classification is less close to our task, making the usage of VGGNet or ResNet, as an image classifier, less reasonable.

The AE monitoring data was processed through short-term Fourier transform (STFT) to generate a 2-dimensional time-frequency spectrum before being sent to the CNN model, and focus was put on the 90–140 kHz range according to the authors' previous research (Liu et al., 2015; Wang et al., 2018). The model is roughly divided into two parts, the low-level layers and the high-level layers. The low-level layers, also denoted as the frozen layers, leverage the knowledge, or more specifically, the well-trained parameters (weight w and bias b) from the source model and output the bottleneck features after multiple layers of ConV-BatchNorm-ReLU-Maxpool cycles, and a multi-layer perceptron (MLP) was used as the high-level layers (trainable layers) to further classify the rail structural condition. The architecture of the model is shown in Fig. 6. The TL process and the data labelling strategy can be viewed in Fig. 7.

The cost was back propagated for parameter updating with the cost function set as:

$$J=\frac{1}{m}\sum_{k=1}^{m}-\left[y^{(k)}\log\hat{y}^{(k)}+\left(1-y^{(k)}\right)\log\left(1-\hat{y}^{(k)}\right)\right] \tag{12}$$

According to research (Chen et al., 2018; Hillmansen and Smith, 2004; Sandström and Ekberg, 2009), fatigue crack grows exponentially, and correspondingly the three-month AE data was divided into four stages (intact, crack initialization, crack expansion, and critically fractured) with AE samples roughly aligned with the stage period. It is worth noting that more stages can be defined as the proposed learning model capable of regressive diagnosis, but four stages were enough to demonstrate the effectiveness.

The model after the proposed acoustic TL, which is denoted as $\mathbf{M_{A\text{-}AE}}$, exhibits excellent performance against the other baseline models $\mathbf{M_{I\text{-}AE}}$, including TL from VGGNet, and ordinary CNN model $\mathbf{M_{AE}}$ learning from

Table 1
Comparisons between MA-AE and baseline model in terms of F1.

	$M_{A\text{-}AE}$	$M_{I\text{-}AE}$	M_{AE}
Stage I	99.9%	98.9%	99.7%
Stage II	96.5%	85.5%	86.0%
Stage III	93.8%	60.2%	64.5%
Stage IV	100.0%	100.0%	99.8%
Average	97.5%	86.1%	87.5%

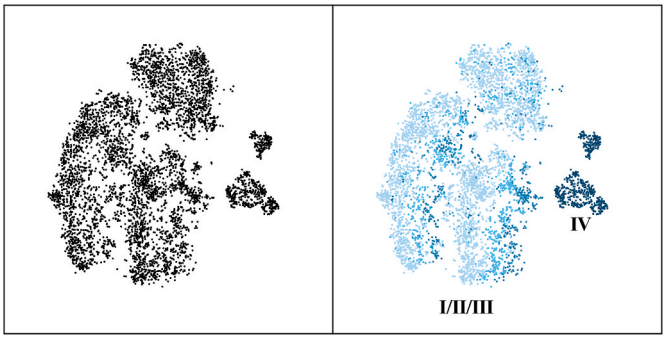

Fig. 8. Visualized features of $M_{I\text{-}AE}$.

scratch in terms of rail condition inference. The F1 core of $\mathbf{M_{A\text{-}AE}}$ is significantly higher than the comparing ones, as shown in Table 1. It can be summarized a proper selection of source model similar to the target tasks can ensure a positive TL. By contrast, knowledge transfer from the image data source may even deteriorate the performance or be noted as negative transfer.

The study dealt with the data limitation issue and enabled regressive diagnosis of the rail health condition by properly transferring knowledge from well-trained and closely related learning models. The visualized 2-dimensional embeddings of the bottleneck features further indicate the potential unsupervised learning capability of the model, as shown on the top left of Fig. 7. It can be found that features from the same rail condition tend to cluster and there exist obvious borders between clusters and subtle trends that reflect the progress of cracks. This result shows that the frozen layers of $\mathbf{M_{A\text{-}AE}}$ can extract meaningful features. For comparison, the features from $\mathbf{M_{I\text{-}AE}}$ are also visualized. In Fig. 8, it can be shown that the features of Stage I to Stage III from $\mathbf{M_{I\text{-}AE}}$ are mixed up, which indicates that the useful information is corrupted by a not-so-relevant model.

With the development of the acoustic-homologous TL approach, the authors' team started to be concerned with the generalization of data-driven models on multiple rail turnouts and rail lines, instead of one or two specific areas. Furthermore, research aiming at improving the TL by cropping the label space is being conducted by the authors and will be elaborated on in the next section.

5. Reliable crack evaluation with TS-guided TL

In essence, TL aims to leverage the knowledge learned from one task for another related task. The former is called source task while the latter is called target task. In our case, the target task $\mathscr{T}_T = \{\mathscr{Y}_T, f_T(\cdot)\}$ is to identify crack based on AE, where $f_T(\cdot)$ is the function to map the AE to the stage of crack and $\mathscr{Y}_T$ indicates the label space of target task, which is four stages of crack.

According to (Pan and Yang, 2010; Wang et al., 2019), TL requires that $\mathscr{T}_S$ and $\mathscr{T}_T$ are similar, otherwise the adoption of TL may deteriorate the performance of TL. In the previous analysis, the TS between source task and target task is only analyzed by intuition. To make it more rigorous, we adopt the idea of representation similarity analysis (RSA) from cognitive science to measure the TSs between the target task and three candidate source tasks. The target task is AE-based crack monitoring while the three source tasks are (1) sound event detection; (2) Image Classification; and (3) Crack-related sound event detection. The calculation of TS for three candidate source models is shown in Fig. 9.

Then, following the same procedures as Section 4, we conducted parameter-based TL by combining a classifier to the low-level layers of source modes within our model for crack identification to combine with a classifier.

The details of calculating RDM and TS are shown in Fig. 10. By inputting the available dataset into target and source models, two representation sets and representation dissimilarity matrices (RDMs) can be

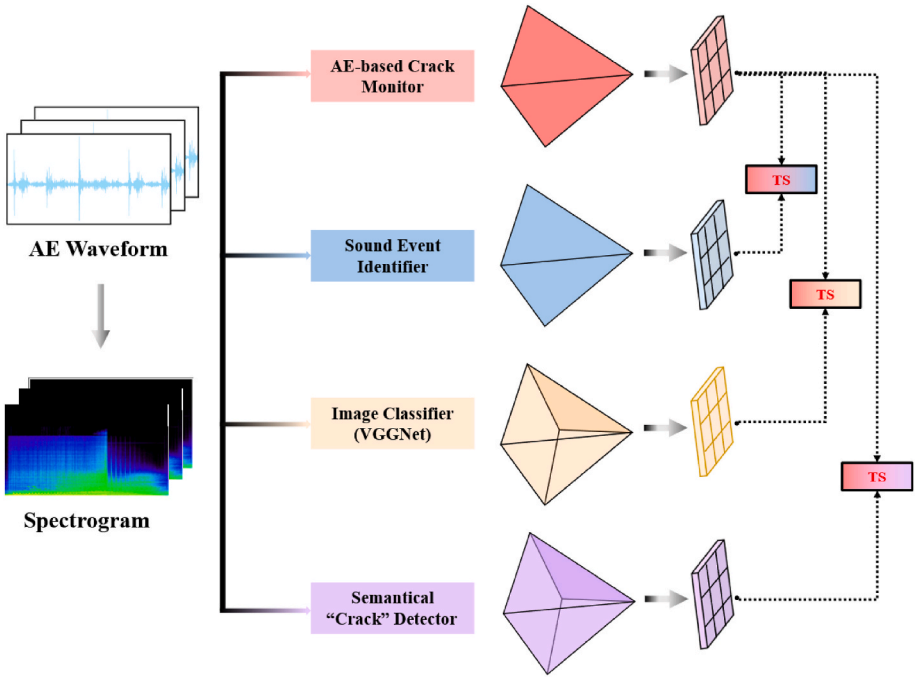

Fig. 9. Illustration of calculating TS between target task and three source tasks.

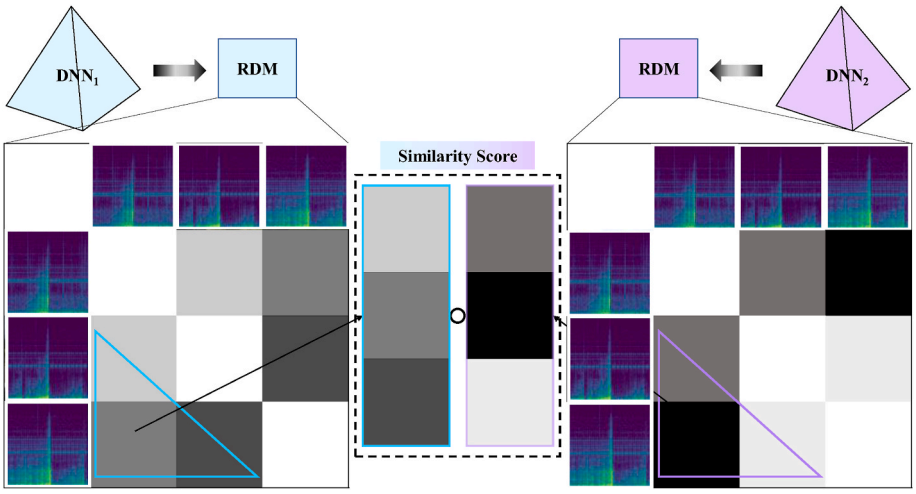

Fig. 10. Details of calculating RDM and TS.

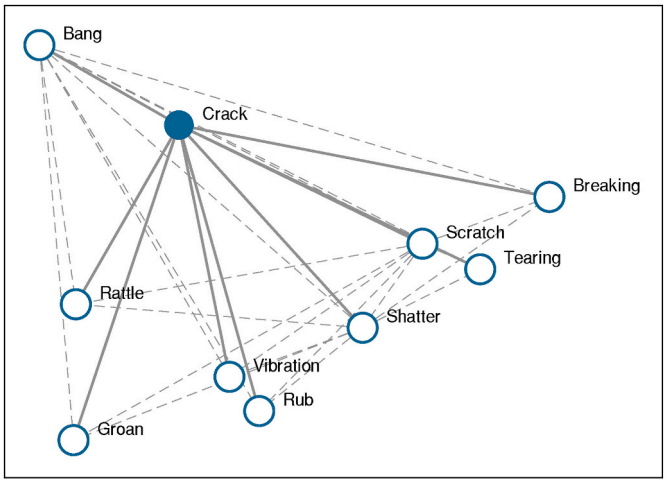

Fig. 11. Top 10 labels that are most related to "crack".

obtained, which contain the similarity scores of each pair of samples. RDM was used as a signature of the representations in computational models since the concept of second-order isomorphism can serve a more general purpose, according to related studies in cognitive science (Shepard and Chipman, 1970). The calculation of TS is:

$$TS = 1 - \frac{6\sum d_i^2}{n(n^2-1)} \tag{13}$$

where d_i is the difference between the ranks of ith elements of the lower triangular part of the two RDMs and n is the number of elements in the lower triangular part of the RDM.

Regarding the source tasks shown in Fig. 9, the source task 1 $\mathscr{T}_{S1} = \{\mathscr{Y}_{S1}, f_{S1}(\cdot)\}$, as mentioned in Section 4 is to sound event detection based on AudioSet (Kumar et al., 2018), where $f_{S1}(\cdot)$ is the function to map sound recordings to the sound event and $\mathscr{Y}_S$ indicates the label space of source task, which is the 527 kind of sound events in the Audioset. The source task 2 is image classification based on VGG-Net and the source task 3 is designed and obtained in the following procedures.

In Section 4, it has been analyzed that $\mathscr{T}_{S1}$ and $\mathscr{T}_T$ are similar in terms of the predictive function $f_{S1}(\cdot)$ because they are all identifying sound events from a noisy background, but in our case, the label space of the source task $\mathscr{Y}_{S1}$ is different from the label space of the target task $\mathscr{Y}_T$ because most sound events in AudioSet are highly unrelated to cracking, breaking, or impacting. To make $\mathscr{T}_S$ more similar to $\mathscr{T}_T$, we further crop the label space of the source task $\mathscr{Y}_S$.

Table 2
Relationship between F1 score after TL and TS between tasks.

	Target Task	Source Task 1	Source Task 2	Source Task 3
TS	N/A	0.379	0.294	0.411
F1 score	87.5%	97.5%	86.1%	98.2%

Specifically, among all 527 labels in AudioSet, we used BERT (Devlin et al., 2018) to calculate the word embedding (Levy and Goldberg, 2014) of each label and calculate their correlations to the word embedding of "crack". The labels with top highest correlations mean that these labels are semantically similar to "crack" and the corresponding signals in the source audio dataset are most likely to be solitary non-stationary signals. Among 527 labels, the 10 labels that are most related to "crack" are "Crack", "Scratch", "Shatter", "Bang", "Vibration", "Tearing", "Breaking", "Rattle", "Groan", and "Rub", and their similarities to "crack" are 1,0.902, 0.899, 0.894, 0.886, 0.881, 0.879, 0.871, 0.870 and 0.869, respectively. To better illustrate the label similarities between each other, we conduct multi-dimensional scaling (MDS) and plot the MDS figure in Fig. 11. The closer the two labels are, the more they are related to each other.

The 636 samples in Audioset corresponding to these labels are selected out as a fine-tuning dataset. The architecture of model for AE classification (as shown in Fig. 6) remains the same with pre-trained parameters but the classifier and Block 7 in the feature extractor are unfrozen. The 636 samples with labels related to "crack" are used to finetune the unfrozen part of the model. In this way, the model was modified to be suitable for the task of crack-related sound event detection, denoted as source task 3, which is more likely to be similar to the target task.

Results show that the TS between the target task and the source task in Section 4 is 0.379, while this value can be improved to 0.411 when the

Table 3
F1 score of samples for each stage after TL from source Task 3.

	F1 score
Stage I	99.9%
Stage II	97.2%
Stage III	95.6%
Stage IV	100%
Average	98.2%

Table 4
Capability of the proposed approaches for AE-based switch rail monitoring.

	Time-frequency analysis	Bayesian framework	Acoustic transfer learning	Semantical crack-related transfer learning
Achievable goal	Binary crack detection	Crack severity classification	Regressive condition assessment	Improved regressive condition assessment
Generalizable capability	No	Weak	Strong	Strong
Data uncertainty	✗	✓	✓	✓
Limited SHM data	✗	✗	✓	✓
Task-oriented	✗	✗	✗	✓

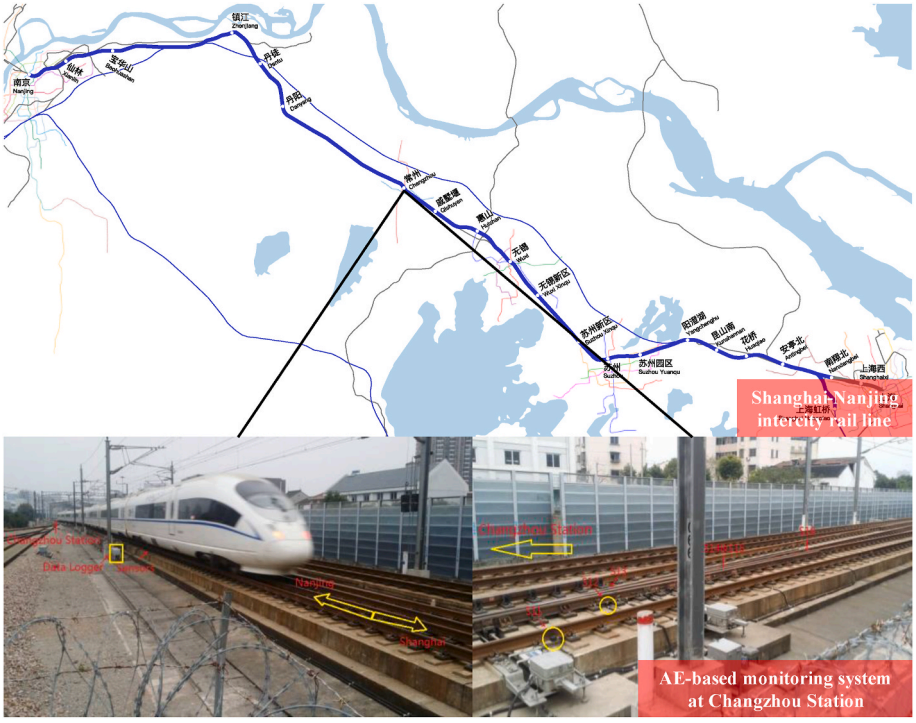

Fig. 12. AE-based rail turnout monitoring system at Changzhou station of Shanghai-Nanjing intercity rail line.

source task is modified by cropping the label space. As shown in Table 2, the higher the TS of the source task, the higher the F1 score can be achieved after TL. In addition, cropping the label space of a source task can help to improve the performance of TL since the task dissimilarity can narrow down.

The model after TL from source model 2 is denoted as $\mathscr{M}_{S3\to T}$ and overall, the macro-F1 of $\mathscr{M}_{S3\to T}$ is 98.2%. For each class, the F1 score is shown in Table 3.

6. Summary and outlooks

The research series covers a long-term SHM project for switch rail in the operating rail line, embracing the state-of-the-art data-driven analysing frameworks, which achieves growing practical applicability of the developed AE-based monitoring system under an open environment with great uncertainty and limited well-labelled samples, enabling real-time condition assessment rather than binary crack detection. Generally speaking, we are seeking a growingly adaptive solution series for AE-based switch rail monitoring in terms of higher diagnosis accuracy and greater generalizable capability. By incorporating TL frameworks, we expect the knowledge and well-trained learning models can be transferred between different rail turnout areas under various operating conditions and rail types. Table 4 briefly summarizes the function of the proposed approaches in terms of achieved goals and arising issues. Through the research series, one may somehow catch a glimpse of the data-driven SHM development over these years, particularly for models with TL, which were still at a pioneering stage in SHM at the year when the authors conceptualized the idea of introducing the framework in our case, are now experiencing flourishing applications in various Civil and Mechanical monitoring scenarios.

Meanwhile, upon the increasing reliability and robustness of both software and hardware, the developed AE-based monitoring system had also been deployed on many other rail turnout areas in multiple operating rail lines apart from the Chengdu North marshalling yard, including No. 8 rail turnout, Line 2 of Changzhou Station on the Shanghai-Nanjing Intercity Rail line (Fig. 12); No. 5, 6, 7, 10 turnouts of

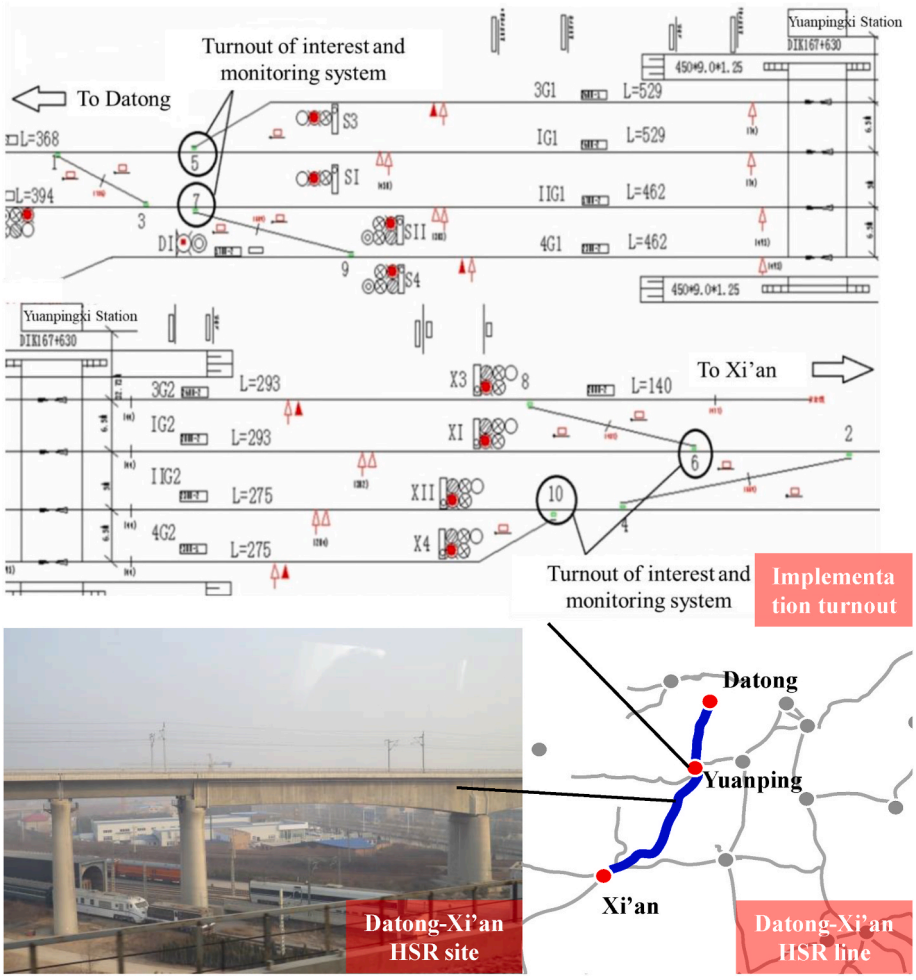

Fig. 13. AE-based rail turnout monitoring system at Yuanpingxi station of Datong-Xi'an HSR line.

Yangquxi Station, No. 9, 10, 14, 15 turnouts of Xinzhouxi Station and No. 5, 6, 9, 10 turnouts of Yuanpingxi Station on the Datong-Xi'an HSR line (Fig. 13); No. 1 and 5 rail turnouts, Xiaotuanshan line on the Shanghai-Kunming HSR line; and No. 18 rail turnout of Qiananbei Station on the Datong-Qinghuangdao freight rail line. The monitoring systems have been working steadily ever since and provided more valuable in-situ monitoring data.

It should be admitted that the AE sensing technique, concerning the high attenuation of AE bursts particularly within the ultrasound range, is applicable in a damage-close area, which is why it is adopted primarily for rail turnout areas normally within a 10m range. However, the proposed method is still extensively applicable. Firstly, for each rail turnout, we only need one sensing element to be implemented in on point rail, which helps to handle the limitation of sensor number. Second, the proposed series of methods are not designed to monitor the whole section railway but only some critical components of the rail, such as turnout in the presented case. For rail turnout whose damage may easily lead to accidents, it is worthwhile to use one sensor for its health condition. The proposed methods are expected to be applicable to other critical components.

In addition, current studies mainly focus on evaluating the health status of one or several rail turnouts. In real engineering practice, there are limited kinds of rail turnout. Therefore, each specific turnout of the same kind can be considered a member drawn from a population of turnout and be simultaneously monitored. This follows the idea of population-based SHM (PBSHM) (Bull et al., 2021; Worden et al., 2020). In this way, the model for rail condition assessment, once trained, can be applied to other turnouts of the same kind, i.e. the rest members of the

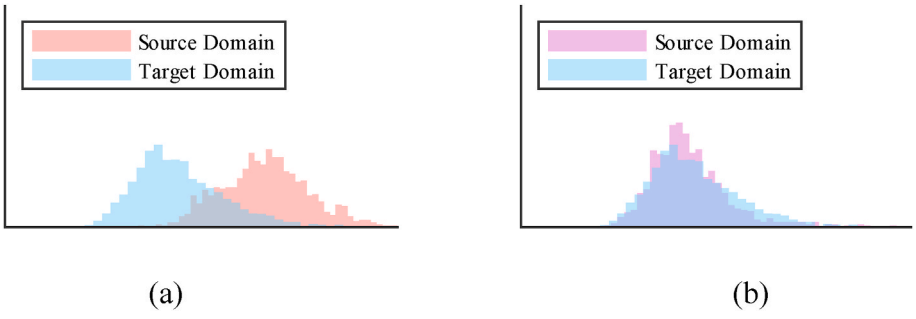

Fig. 14. Data distribution from different operational environments: (a). before domain adaptation; (b) after domain adaptation.

same population, which helps to improve the reliability of the railway systems from a system perspective rather than just a component perspective. Despite this advantage, one issue to be resolved is the variation of operational environment. Each kind of turnout may be used for different rail sections at different locations and both the environmental factors (temperature, soil condition, wind etc.) and rail infrastructures (track bed, rail foundations, etc.) can be quite different, leading to the shift of AE data distribution and thus the performance decay of rail condition evaluation model. We plan to introduce domain adaption (Chen et al., 2022; Wilson and Cook, 2020) to handle this issue by aligning the distribution of data collected at different rail turnouts as illustrated in Fig. 14. It is expected that the model, after domain adaptation can be more generalizable and more suitable for simultaneous monitoring turnouts within the same population.

CRediT authorship contribution statement

Lu Zhou: Writing – original draft, Visualization, Methodology, Investigation, Formal analysis. **Si-Xin Chen:** Writing – review & editing, Visualization, Validation, Software, Investigation, Conceptualization. **Yi-Qing Ni:** Writing – review & editing, Supervision, Project administration, Funding acquisition, Conceptualization. **Xiao-Zhou Liu:** Visualization, Resources, Methodology, Investigation, Data curation.

Declaration of competing interest

The authors declare that they have no known competing financial interests or personal relationships that could have appeared to influence the work reported in this paper.

Acknowledgements

The corresponding author would like to acknowledge the STU Scientific Research Initiation Grant from Shantou University, grant number NTF23009. This research also was funded by a grant from the Innovation and Technology Commission of Hong Kong SAR Government to the Hong Kong Branch of Chinese National Rail Transit Electrification and Automation Engineering Technology Research Center, grant number K-BBY1.

References

Ahmadzadeh, M., Zahrai, S.M., Bitaraf, M., 2024. An integrated deep neural network model combining 1D CNN and LSTM for structural health monitoring utilizing multisensor time-series data. Struct. Health Monit. https://doi.org/10.1177/14759217241239041.

Anandika, R., Lundberg, J., Stenström, C., 2020. Phased array ultrasonic inspection of near-surface cracks in a railhead and its verification with rail slicing. Insight-Non-Destructive Testing and Condition Monitoring 62 (7), 387–395. https://doi.org/10.1784/insi.2020.62.7.387.

Barile, C., Casavola, C., Pappalettera, G., Kannan, V.P., 2022. Damage monitoring of carbon fibre reinforced polymer composites using acoustic emission technique and deep learning. Compos. Struct. 292, 115629. https://doi.org/10.1016/j.compstruct.2022.115629.

Bartoli, I., Lanza di Scalea, F., Fateh, M., Viola, E., 2005. Modeling guided wave propagation with application to the long-range defect detection in railroad tracks. NDT E Int 38 (5), 325–334. https://doi.org/10.1016/j.ndteint.2004.10.008.

Bartoli, I., Marzani, A., Di Scalea, F.L., Viola, E., 2006. Modeling wave propagation in damped waveguides of arbitrary cross-section. J. Sound Vib. 295 (3–5), 685–707. https://doi.org/10.1016/j.jsv.2006.01.021.

Benzeroual, H., Khamlichi, A., Zakriti, A., 2021. Inspection of transverse flaws for railways using phased array ultrasonic technique. Int. Rev. App. Sci.Eng. 12 (2), 119–126. https://doi.org/10.1556/1848.2020.00187.

Bruzelius, K., Mba, D., 2004. An initial investigation on the potential applicability of Acoustic Emission to rail track fault detection. NDT E Int 37 (7), 507–516. https://doi.org/10.1016/j.ndteint.2004.02.001.

Bull, L.A., Gardner, P.A., Dervilis, N., Papatheou, E., Haywood-Alexander, M., Mills, R.S., Worden, K., 2021. On the transfer of damage Detectors between structures: an experimental case study. J. Sound Vib. 501, 116072. https://doi.org/10.1016/j.jsv.2021.116072.

Chen, J., Yuan, S., Qiu, L., Wang, H., Yang, W., 2018. On-line prognosis of fatigue crack propagation based on Gaussian weight-mixture proposal particle filter. Ultrasonics 82, 134–144. https://doi.org/10.1016/j.ultras.2017.07.016.

Chen, R., Hu, C., Xu, J., Gong, Z., Liu, L., Wang, P., Chen, X., 2021a. Research on guided wave propagation characteristics in turnout rails with variable cross-section. J. Sound Vib. 494, 115853. https://doi.org/10.1016/j.jsv.2020.115853.

Chen, S.X., Zhou, L., Ni, Y.Q., 2022. Wheel condition assessment of high-speed trains under various operational conditions using semi-supervised adversarial domain adaptation. Mech. Syst. Signal Process. 170, 108853. https://doi.org/10.1016/j.ymssp.2022.108853.

Chen, S.X., Zhou, L., Ni, Y.Q., Liu, X.Z., 2021b. An acoustic-homologous transfer learning approach for acoustic emission–based rail condition evaluation. Struct. Health Monit. 20 (4), 2161–2181. https://doi.org/10.1177/1475921720976941.

Coccia, S., Bartoli, I., Marzani, A., di Scalea, F.L., Salamone, S., Fateh, M., 2011. Numerical and experimental study of guided waves for detection of defects in the rail head. NDT E Int 44 (1), 93–100. https://doi.org/10.1016/j.ndteint.2010.09.011.

Devlin, J., Chang, M.-W., Lee, K., Toutanova, K., 2018. Bert: pre-training of deep bidirectional transformers for language understanding. ArXiv Preprint. ArXiv: 1810.04805. https://doi.org/10.48550/arXiv.1810.04805.

di Scalea, F.L., McNamara, J., 2003. Ultrasonic NDE of railroad tracks: air-coupled cross-sectional inspection and long-range inspection. Insight-Non-Destructive Testing and Condition Monitoring 45 (6), 394–401. http://doi.org/10.1784/INSI.45.6.394.52890.

di Scalea, F.L., McNamara, J., 2004. Measuring high-frequency wave propagation in railroad tracks by joint time–frequency analysis. J. Sound Vib. 273 (3), 637–651. https://doi.org/10.1016/S0022-460X(03)00563-7.

Dimsumdaily Hong Kong, 2019. Experts express that the cause of the derailment is potentially due to cracked railway track. Dimsun Daily. https://www.dimsumdaily.hk/experts-express-that-the-cause-of-the-derailment-is-potentially-due-to-cracked-railway-track.

Elforjani, M., Shanbr, S., 2017. Prognosis of bearing acoustic emission signals using supervised machine learning. IEEE Trans. Ind. Electron. 65 (7), 5864–5871. https://doi.org/10.1109/TIE.2017.2767551.

Fan, Y., Dixon, S., Edwards, R.S., Jian, X., 2007. Ultrasonic surface wave propagation and interaction with surface defects on rail track head. NDT E Int 40 (6), 471–477. https://doi.org/10.1063/1.2184714.

Figueiredo, E., Omori Yano, M., Da Silva, S., Moldovan, I., Adrian Bud, M., 2023. Transfer learning to enhance the damage detection performance in bridges when using numerical models. J. Bridge Eng. 28 (1), 4022134. https://doi.org/10.1061/(ASCE)BE.1943-5592.0001979.

Ge, H., Chua Kim Huat, D., Koh, C.G., Dai, G., Yu, Y., 2022. Guided wave–based rail flaw detection technologies: state-of-the-art review. Struct. Health Monit. 21 (3), 1287–1308. https://doi.org/10.1177/14759217211013110.

Gemmeke, J.F., Ellis, D.P.W., Freedman, D., Jansen, A., Lawrence, W., Moore, R.C., Plakal, M., Ritter, M.. Audio set: an ontology and human-labeled dataset for audio events. https://doi.org/10.1109/ICASSP.2017.7952261.

Han, G., Kim, Y.M., Kim, H., Oh, T.M., Song, K.I., Kim, A., Kim, Y., Cho, Y., Kwon, T.H., 2021. Auto-detection of acoustic emission signals from cracking of concrete structures using convolutional neural networks: upscaling from specimen. Expert Syst. Appl. 186, 115863. https://doi.org/10.1016/j.eswa.2021.115863.

Hao, Q., Shen, Y., Wang, Y., Liu, J., 2021. An adaptive extraction method for rail crack acoustic emission signal under strong wheel-rail rolling noise of high-speed railway. Mech. Syst. Signal Process. 154, 107546. https://doi.org/10.1016/j.ymssp.2020.107546.

Hillmansen, S., Smith, R.A., 2004. The management of fatigue crack growth in railway axles. Proc. Inst. Mech. Eng. F J. Rail Rapid Transit 218 (4), 327–336. https://doi.org/10.1243/0954409043125879.

Hu, S., Shi, W., Lu, C., Chen, Y., Chen, G., Shen, G., 2021. Rapid detection of cracks in the rail foot by ultrasonic B-scan imaging using a shear horizontal guided wave electromagnetic acoustic transducer. NDT E Int 120, 102437. https://doi.org/10.1016/j.ndteint.2021.102437.

Jaramillo, F., Gutiérrez, J.M., Orchard, M., Guarini, M., Astroza, R., 2022. A Bayesian approach for fatigue damage diagnosis and prognosis of wind turbine blades. Mech. Syst. Signal Process. 174, 109067. https://doi.org/10.1016/j.ymssp.2022.109067.

Khodabandehlou, H., Pekcan, G., Fadali, M.S., 2019. Vibration-based structural condition assessment using convolution neural networks. Struct. Control Health Monit. 26 (2), e2308. https://doi.org/10.1002/stc.2308.

Kim, G., Seo, M.-K., Kim, Y.-I., Kwon, S., Kim, K.-B., 2020. Development of phased array ultrasonic system for detecting rail cracks. Sensor Actuator Phys 311, 112086. https://doi.org/10.1016/j.sna.2020.112086.

Kongpuang, M., Culwick, R., Cheputeh, N., Marsh, A., Jantara Junior, V.L., Vallely, P., Kaewunruen, S., Papaelias, M., 2022. Quantitative analysis of the structural health of railway turnouts using the acoustic emission technique. Insight-Non-Destructive Testing and Condition Monitoring 64 (7), 398–403. https://doi.org/10.1784/insi.2022.64.7.398.

Kumar, A., Khadkevich, M., Fugen, C., Fügen, C., 2018. Knowledge transfer from weakly labeled audio using convolutional neural network for sound events and scenes. In: 2018 IEEE International Conference on Acoustics, Speech and Signal Processing (ICASSP), pp. 326–330. https://doi.org/10.1109/ICASSP.2018.8462200.

Levy, O., Goldberg, Y., 2014. Neural word embedding as implicit matrix factorization. Adv. Neural Inf. Process. Syst. 27, 2177–2185.

Li, D., Yang, W., Zhang, W., 2017. Cluster analysis of stress corrosion mechanisms for steel wires used in bridge cables through acoustic emission particle swarm optimization. Ultrasonics 77, 22–31. https://doi.org/10.1016/j.ultras.2017.01.012.

Li, M., Jia, D., Wu, Z., Qiu, S., He, W., 2022. Structural damage identification using strain mode differences by the iFEM based on the convolutional neural network (CNN). Mech. Syst. Signal Process. 165, 108289. https://doi.org/10.1016/j.ymssp.2021.108289.

Li, X., Wu, B., Gao, X., Liu, Y., Wang, H., Liu, X., 2023. Ultrasonic SH guided wave detection of the defects of switch rails with 3D finite element method. Measurement 220, 113325. https://doi.org/10.1016/j.measurement.2023.113325.
Li, Y., Xu, F., 2022. Structural damage monitoring for metallic panels based on acoustic emission and adaptive improvement variational mode decomposition–wavelet packet transform. Struct. Health Monit. 21 (2), 710–730. https://doi.org/10.1177/14759217211008969.
Liu, X.Z., Ni, Y.Q., Wu, W.L., Pei, Y.F., Hou, Y.H., Qin, D.Y., 2015. AET-Based pattern recognition technique for rail defect detection. Proc. Struct. Health Monit. 39 (5), 561–563. https://doi.org/10.12783/SHM2015/252.
Loveday, P.W., 2009. Semi-analytical finite element analysis of elastic waveguides subjected to axial loads. Ultrasonics 49 (3), 298–300. https://doi.org/10.1016/j.ultras.2008.10.018.
Loveday, P.W., 2012. Guided wave inspection and monitoring of railway track. J. Nondestr. Eval. 31 (4), 303–309. https://doi.org/10.1007/s10921-012-0145-9.
Loveday, P.W., Long, C.S., Ramatlo, D.A., 2018. Mode repulsion of ultrasonic guided waves in rails. Ultrasonics 84, 341–349. https://doi.org/10.1016/j.ultras.2017.11.014.
Loveday, P.W., Long, C.S., Ramatlo, D.A., 2020. Ultrasonic guided wave monitoring of an operational rail track. Struct. Health Monit. 19 (6), 1666–1684. https://doi.org/10.1177/1475921719893887.
Mao, Z., Todd, M.D., 2016. A Bayesian recursive framework for ball-bearing damage classification in rotating machinery. Struct. Health Monit. 15 (6), 668–684. https://doi.org/10.1177/1475921716656123.
Mariani, S., di Scalea, F.L., 2018. Predictions of defect detection performance of air-coupled ultrasonic rail inspection system. Struct. Health Monit. 17 (3), 684–705. https://doi.org/10.1177/1475921717715429.
Mariani, S., Nguyen, T., Phillips, R.R., Kijanka, P., Lanza di Scalea, F., Staszewski, W.J., Fateh, M., Carr, G., 2013. Noncontact ultrasonic guided wave inspection of rails. Struct. Health Monit. 12 (5–6), 539–548. https://doi.org/10.1177/1475921713498533.
Ng, K., Ghafoor, I., Tse, P., 2022. A novel laser-based duffing oscillator system to identify weak ultrasonic guided wave signals related to rail defects. Opt Laser. Eng. 157, 107111. https://doi.org/10.1016/j.optlaseng.2022.107111.
Ni, Y.Q., Chen, R., 2021. Strain monitoring based bridge reliability assessment using parametric Bayesian mixture model. Eng. Struct. 226, 111406. https://doi.org/10.1016/j.engstruct.2020.111406.
Ni, Y.Q., Wang, Y.W., Zhang, C., 2020. A Bayesian approach for condition assessment and damage alarm of bridge expansion joints using long-term structural health monitoring data. Eng. Struct. 212, 110520. https://doi.org/10.1016/j.engstruct.2020.110520.
Ni, Y.Q., Zhang, Q.H., 2020. A Bayesian machine learning approach for online detection of railway wheel defects using track-side monitoring. Struct. Health Monit. 20 (4), 1536–1550. https://doi.org/10.1177/1475921720921772.
Nielsen, J.S., Tcherniak, D., Ulriksen, M.D., 2021. A case study on risk-based maintenance of wind turbine blades with structural health monitoring. Struct. Infrastruct. Eng. 17 (3), 302–318. https://doi.org/10.1080/15732479.2020.1743326.
Pan, Q., Bao, Y., Li, H., 2023. Transfer learning-based data anomaly detection for structural health monitoring. Struct. Health Monit. 22 (5), 3077–3091. https://doi.org/10.1177/14759217221142174.
Pan, S.J., Yang, Q., 2010. A survey on transfer learning. IEEE Trans. Knowl. Data Eng. 22 (10), 1345–1359. https://doi.org/10.1109/TKDE.2009.191.
Rai, A., Mitra, M., 2022. A transfer learning approach for damage diagnosis in composite laminated plate using Lamb waves. Smart Mater. Struct. 31 (6), 65002. https://doi.org/10.1088/1361-665X/ac66aa.
Ramatlo, D.A., Wilke, D.N., Loveday, P.W., 2018. Development of an optimal piezoelectric transducer to excite guided waves in a rail web. NDT E Int 95, 72–81. https://doi.org/10.1016/j.ndteint.2018.02.002.
Rubio-González, C., de Urquijo-Ventura, M., del, P., Rodríguez-González, J.A., 2023. Damage progression monitoring using self-sensing capability and acoustic emission on glass fiber/epoxy composites and damage classification through principal component analysis. Compos. B Eng. 254, 110608. https://doi.org/10.1016/j.compositesb.2023.110608.
Sandström, J., Ekberg, A., 2009. Predicting crack growth and risks of rail breaks due to wheel flat impacts in heavy haul operations. Proc. Inst. Mech. Eng. F J. Rail Rapid Transit 223 (2), 153–161. https://doi.org/10.1243/09544097JRRT224.
Sawant, S., Sethi, A., Banerjee, S., Tallur, S., 2023. Unsupervised learning framework for temperature compensated damage identification and localization in ultrasonic guided wave SHM with transfer learning. Ultrasonics 130, 106931. https://doi.org/10.1016/j.ultras.2023.106931.
Seventekidis, P., Giagopoulos, D., Arailopoulos, A., Markogiannaki, O., 2020. Structural Health Monitoring using deep learning with optimal finite element model generated data. Mech. Syst. Signal Process. 145, 106972. https://doi.org/10.1016/j.ymssp.2020.106972.
Shepard, R.N., Chipman, S., 1970. Second-order isomorphism of internal representations: shapes of states. Cognit. Psychol 1 (1), 1–17. https://doi.org/10.1016/0010-0285(70)90002-2.
Sony, S., Dunphy, K., Sadhu, A., Capretz, M., 2021. A systematic review of convolutional neural network-based structural condition assessment techniques. Eng. Struct. 226, 111347. https://doi.org/10.1016/j.engstruct.2020.111347.
Sousa, H., Rozsas, A., Slobbe, A., Courage, W., 2020. A novel pro-active approach towards SHM-based bridge management supported by FE analysis and Bayesian methods. Struct. Infrastruct. Eng. 16 (2), 233–246. https://doi.org/10.1080/15732479.2019.1649287.
The Associated Press, 2021. High-speed train services in UK disrupted after cracks found. Seattle Times (WA). https://www.seattletimes.com/business/high-speed-train-services-in-uk-disrupted-after-cracks-found.
Utrata, D., 2002. Exploring enhanced rail flaw detection using ultrasonic phased array inspection. AIP Conf. Proc. 615 (1), 1813–1818. https://doi.org/10.1063/1.1473013.
Wang, C., Gao, J., Li, H., Lin, C., Beck, J.L., Huang, Y., 2023a. Robust sparse Bayesian learning for broad learning with application to high-speed railway track monitoring. Struct. Health Monit. 22 (2), 1256–1272. https://doi.org/10.1177/14759217221104224.
Wang, J., Liu, X.-Z., Ni, Y.-Q., 2018. A bayesian probabilistic approach for acoustic emission-based rail condition assessment. Comput. Aided Civ. Infrastruct. Eng. 33 (1), 21–34. https://doi.org/10.1111/mice.12316.
Wang, K., Cao, W., Xu, L., Yang, X., Su, Z., Zhang, X., Chen, L., 2020a. Diffuse ultrasonic wave-based structural health monitoring for railway turnouts. Ultrasonics 101, 106031. https://doi.org/10.1016/j.ultras.2019.106031.
Wang, W., Sun, Q., Zhao, Z., Sun, X., Qin, F., Kho, K., Zheng, Y., 2023b. Laser-induced ultrasonic guided waves based corrosion diagnosis of rail foot. IEEE Trans. Instrum. Meas. 72, 1–9. https://doi.org/10.1109/TIM.2023.3269125.
Wang, Y.W., Ni, Y.Q., Wang, X., 2020b. Real-time defect detection of high-speed train wheels by using Bayesian forecasting and dynamic model. Mech. Syst. Signal Process. 139, 106654. https://doi.org/10.1016/j.ymssp.2020.106654.
Wang, Y.W., Zhang, C., Ni, Y.Q., Xu, X.Y., 2022. Bayesian probabilistic assessment of occupant comfort of high-rise structures based on structural health monitoring data. Mech. Syst. Signal Process. 163, 108147. https://doi.org/10.1016/j.ymssp.2021.108147.
Wang, Z., Dai, Z., Póczos, B., Carbonell, J.. Characterizing and avoiding negative transfer. https://doi.org/10.1109/CVPR.2019.01155.
Wilson, G., Cook, D.J., 2020. A survey of unsupervised deep domain adaptation. ACM Trans. Intell. Syst. Technol. 11 (5), 1–46. https://doi.org/10.1145/3400066.
Worden, K., Bull, L.A., Gardner, P., Gosliga, J., Rogers, T.J., Cross, E.J., Papatheou, E., Lin, W., Dervilis, N., 2020. A Brief Introduction to Recent Developments in Population-Based Structural Health Monitoring. Front. Built Environ. 6, 1–14. https://doi.org/10.3389/fbuil.2020.00146.
Wu, J., Tang, Z., Lv, F., Yang, K., Yun, C.B., Duan, Y., 2018. Ultrasonic guided wave-based switch rail monitoring using independent component analysis. Meas. Sci. Technol. 29 (11), 115102. https://doi.org/10.1088/1361-6501/aadc47.
Wu, Y., Li, S., 2022. Damage degree evaluation of masonry using optimized SVM-based acoustic emission monitoring and rate process theory. Measurement 190, 110729. https://doi.org/10.1016/j.measurement.2022.110729.
Xu, C., Du, S., Gong, P., Li, Z., Chen, G., Song, G., 2020. An improved method for pipeline leakage localization with a single sensor based on modal acoustic emission and empirical mode decomposition with Hilbert transform. IEEE Sens. J. 20 (10), 5480–5491. https://doi.org/10.1109/JSEN.2020.2971854.
Xu, J., Liu, X., Han, Q., Wang, W., 2021a. A particle swarm optimization–support vector machine hybrid system with acoustic emission on damage degree judgment of carbon fiber reinforced polymer cables. Struct. Health Monit. 20 (4), 1551–1562. https://doi.org/10.1177/1475921720922824.
Xu, J., Wang, P., An, B., Chen, R., Xiao, J., Liang, W., Hou, Y., 2017. Acoustic emission monitoring of switch rail detect based on Wigner-Ville high-order spectrum and data mining technology. In: Proceedings of the 2017 World Congress on Advances in Structural Engineering and Mechanics (ASEM 17), Korea.
Xu, S., Peng, C., Guo, J., Peng, J., Luo, L., 2021b. Denoising of phased array ultrasonic total focus image on rail bottom welds. In: 2021 IEEE Far East NDT New Technology & Application Forum (FENDT), pp. 73–77. https://doi.org/10.1109/FENDT54151.2021.9749663.
Ye, X., Ni, Y.-Q., Ao, W.K., Yuan, L., 2024. Modeling of the hysteretic behavior of nonlinear particle damping by Fourier neural network with transfer learning. Mech. Syst. Signal Process. 208, 111006. https://doi.org/10.1016/j.ymssp.2023.111006.
Ye, X., Ni, Y.-Q., Sajjadi, M., Wang, Y.-W., Lin, C.-S., 2022. Physics-guided, data-refined modeling of granular material-filled particle dampers by deep transfer learning. Mech. Syst. Signal Process. 180, 109437. https://doi.org/10.1016/j.ymssp.2022.109437.
Zeng, J., Todd, M.D., Hu, Z., 2023. Probabilistic damage detection using a new likelihood-free Bayesian inference method. J. Civ. Struct. Health Monit. 13 (2), 319–341. https://doi.org/10.1007/s13349-022-00638-5.
Zhang, F.L., Xiong, H.B., Shi, W.X., Ou, X., 2016a. Structural health monitoring of Shanghai Tower during different stages using a Bayesian approach. Struct. Control Health Monit. 23 (11), 1366–1384. https://doi.org/10.1002/stc.1840.
Zhang, H., Lin, J., Hua, J., Gao, F., Tong, T., 2022. Data anomaly detection for bridge SHM based on CNN combined with statistic features. J. Nondestr. Eval. 41 (1), 28. https://doi.org/10.1007/s10921-022-00857-2.
Zhang, J., Ma, H., Yan, W., Li, Z., 2016b. Defect detection and location in switch rails by acoustic emission and Lamb wave analysis: a feasibility study. Appl. Acoust. 105, 67–74. https://doi.org/10.1016/j.apacoust.2015.11.018.
Zhang, X., Feng, N., Wang, Y., Shen, Y., 2014. An analysis of the simulated acoustic emission sources with different propagation distances, types and depths for rail defect detection. Appl. Acoust. 86, 80–88. https://doi.org/10.1016/j.apacoust.2014.06.004.
Zhang, X., Feng, N., Wang, Y., Shen, Y., 2015. Acoustic emission detection of rail defect based on wavelet transform and Shannon entropy. J. Sound Vib. 339, 419–432. https://doi.org/10.1016/j.jsv.2014.11.021.
Zhang, X., Sun, T., Wang, Y., Wang, K., Shen, Y., 2021. A parameter optimized variational mode decomposition method for rail crack detection based on acoustic emission technique. Nondestr. Test. Eval. 36 (4), 411–439. https://doi.org/10.1080/10589759.2020.1785447.